

First-principles determination of the Raman fingerprint of rhombohedral graphite

Abderrezak Torche,^{1,*} Francesco Mauri,^{2,3,†} Jean-Christophe Charlier,^{4,‡} and Matteo Calandra^{1,§}

¹*IMPMC, CNRS, Université P. et M. Curie, 4 Place Jussieu, 75005 Paris, France*

²*Departmento di Fisica, Università di Roma La Sapienza, Piazzale Aldo Moro 5, I-00185 Roma, Italy*

³*Graphene Labs, Fondazione Istituto Italiano di Tecnologia, Via Morego, I-16163 Genoa, Italy*

⁴*Université catholique de Louvain, Institute of Condensed Matter and Nanosciences, Chemin des étoiles 8, 1348 Louvain-la-Neuve, Belgium*

(Received 2 June 2017; published 18 September 2017)

Multilayer graphene with rhombohedral stacking is a promising carbon phase possibly displaying correlated states like magnetism or superconductivity due to the occurrence of a flat surface band at the Fermi level. Recently, flakes of thickness up to 17 layers were tentatively attributed to ABC sequences although the Raman fingerprint of rhombohedral multilayer graphene is currently unknown and the 2D resonant Raman spectrum of Bernal graphite is not understood. We provide a first principles description of the 2D Raman peak in three and four layers graphene (all stackings) as well as in Bernal, rhombohedral, and an alternation of Bernal and rhombohedral graphite. We give practical prescriptions to identify long range sequences of ABC multilayer graphene. Our work is a prerequisite to experimental nondestructive identification and synthesis of rhombohedral graphite.

DOI: 10.1103/PhysRevMaterials.1.041001

Bernal graphite [1] with AB stacked graphene is the most stable form of graphite. Recently, however, rhombohedral stacked multilayers graphene (RMG) with ABC stacking, see Fig. 1(a), attracted increasing attention as theoretical calculations suggest the occurrence of a dispersionless electronic band (bandwidth smaller than 2 meV) at the Fermi level [2]. This flat band with extremely large effective mass constitutes a very promising candidate for highly correlated states of matter such as magnetism [3] or room-temperature superconductivity [4].

As ABC-stacked graphite is metastable [5], the synthesis of long sequences of ABC graphene layers is a real challenge. For a random sequence of N graphene layers stacked along the c axis, a purely statistical argument states that the probability to obtain N layers with ABC order is $1/2^{N-1}$. In reality the probability is even lower as all stackings are not equally probable as energetics favor the Bernal one with respect to the others. This explains why three and four layer graphene flakes with ABC stacking are systematically found [6–8], while it is highly improbable to obtain long range ABC-stacking order. Recently, it has been suggested that pentlayers graphene with rhombohedral stacking can be grown epitaxially on 3C-SiC(111) [9]. Finally, Henni *et al.* [10] were able to isolate multilayer graphene flakes with ABC sequences exceeding 17 graphene sheets. However, while for three and four ABC stacked graphene layers an optical signature exists [6,7], a clear fingerprint of long-range rhombohedral order is lacking.

Raman spectroscopy, and in particular the 2D double resonant Raman peak, has proven to be a very powerful technique to investigate structural and physical properties of graphene flakes. It can be used to count the number of layers [11], detect charged impurities [12], measure the strain-induced deformation of the electronic structure [13,14], measure the phonon dispersion [15,16], and many other properties (for a review see Ref. [17]). However, despite its

crucial importance, the theoretical understanding of the 2D double resonant Raman spectrum has been obtained only for graphene [18–20] and bilayer graphene [16]. Even the basic case of bulk Bernal graphite is not completely understood. In this Rapid Communication we provide a complete first principles description of the 2D Raman peak in three and four layer graphene for all possible stackings, as well as for bulk AB, bulk ABC, and a periodic mixing of the two (the so-called ABCB graphite). We present calculations for several laser energies and we give practical prescriptions to identify long sequences of ABC stacked multilayer graphene.

Double resonant spectra are calculated from first principles using the method developed in Ref. [16]. The electrons and phonons bands were first calculated by using the QUANTUM ESPRESSO [22] code in the local density approximation with norm-conserving pseudopotentials and an energy cutoff of 70 Ry. Electronic integration was performed on k -point grids of 64×64 for three and four layer systems and $64 \times 64 \times 4$ for Bernal graphite. For rhombohedral graphite we use the hexagonal unit cell containing three layers (6 atoms/unit cell) and a $64 \times 64 \times 4$ k -point grid. The dynamical matrices and the electron-phonon coupling were first calculated in linear response on sparse phonon momentum grids (6×6 for three and four layer graphene and $6 \times 6 \times 3$ for bulk graphites) and then both were Wannier interpolated throughout the Brillouin zone (BZ) using the method of Ref. [23]. We use the LDA+GW approximation both for the electronic bands and the phonon frequencies, as performed in Ref. [16]. The double resonant Raman cross section was calculated on ultradense phonon grids for reciprocal space integration, namely, grids of 300×300 for three and four layers and up to $300 \times 300 \times 16$ for bulk graphites and electron grids as large as 256×256 for few layers and $128 \times 128 \times 16$ for bulk graphites. As only a small percentage of the phonon and electron momenta in the grids actually contributes to the cross section, we develop an automatic technique to identify the subset of relevant points (see Ref. [24]). The electron lifetime was chosen as in Ref. [16] and it was kept the same for all calculations.

We first calculate the double resonant Raman spectra for three and four layers, where a determination of the stacking

*abderrezak.torche@upmc.fr

†francesco.mauri@uniroma1.it

‡jean-christophe.charlier@uclouvain.be

§matteo.calandra@upmc.fr

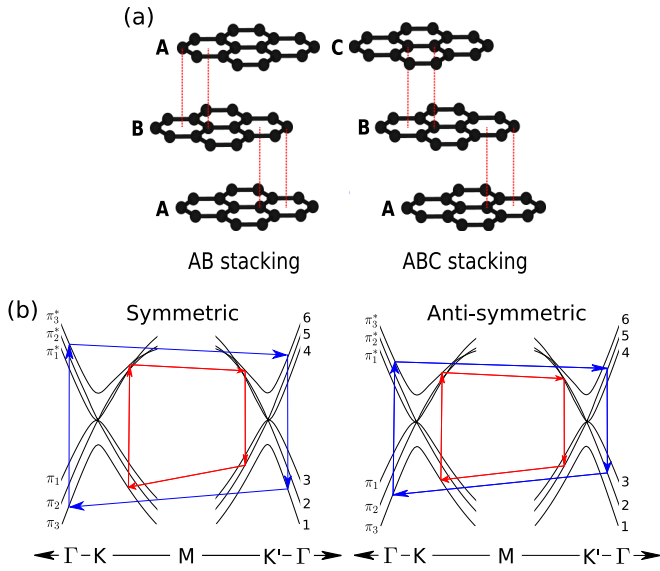


FIG. 1. (a) Crystal structure of Bernal (ABA) and rhombohedral (ABC) stacked multilayer graphene. (b) Cartoon of symmetric, asymmetric, inner (red), and outer (blue) double resonant Raman processes in trilayer graphene.

sequence has been obtained by optical measurements [7]. The results are shown in Fig. 2 for three layers and several laser energies and in Fig. 3 for four layers. Additional results for the four-layers case are presented in the Supplemental Material [24]. Overall we find a good agreement between our parameter-free *ab initio* calculation and experimental data. We reproduce all spectral features in position, width, and intensities as well as the laser energy dependence of the spectra. Our results show that the spectra differ from one stacking to the other. This is mostly due to the difference in electronic structure between different stackings and to the dominance of symmetric inner processes (see Fig. 1(b) and Supplemental Material [24]). Indeed, while along the Γ -K direction, the electronic structure is stacking independent for

both three and four layers, it differs along the \mathbf{K} -M high symmetry line. As a consequence, electron-hole pairs are created/destroyed at slightly different points in the BZ for the same incident laser energy. As shown in Fig. 1(b), inner processes imply electron-hole pairs creation and distraction in the BZ region close to \mathbf{K} -M-K and thus the resulting spectrum mostly feel the difference in electronic structure close to this high symmetry direction. A similar effect occurs in four layer graphene (see Fig. 3). Having validated our calculation against experimental data on three and four layers graphene, we switch to the case of bulk graphite. We first consider bulk AB graphite (Bernal graphite) for which several experimental data are available. We calculate the spectra for different laser energies finding a good agreement with experimental data (see Fig. 4). We then consider in more details the spectra at $\omega_L = 1.96$ eV. The 2D peak is composed of a main peak at ≈ 2683 cm^{-1} and a shoulder around 2640 cm^{-1} , as shown in Fig. 4. Both features are well described by the calculation. The shape and intensities of the D+D'' overtone structure at ≈ 2456 cm^{-1} , although at slightly lower energy in the calculation, are also well reproduced.

In order to detect signatures of different kinds of stackings, we perform calculations for the case of ABC bulk graphite and ABCB bulk graphite. ABCB bulk graphite is interesting as it corresponds to a sequence \dots [ABC](BAB)[CBA](BCB) \dots that is an equal mixing of trilayers with rhombohedral (labeled [ABC or CBA]) and Bernal (labeled (BAB or BCB)) stackings. Thus, the differences between bulk AB and ABCB stackings can be seen as a fingerprint of local rhombohedricity (i.e., few ABC layers) while the differences between bulk ABCB and bulk ABC are signatures of long range rhombohedral order. The results are depicted in Fig. 5, where they are compared with the spectrum of Ref. [10] that has been tentatively attributed to 17 layers ABC-stacked graphene. Both the 2D peaks spectra of bulk ABC and ABCB graphite are substantially broader than the one of Bernal graphite.

Even if both bulk ABC and bulk ABCB spectra seems similar, they differ for the presence of a feature at ≈ 2560 cm^{-1} in the ABC case that is completely missing in the ABCB

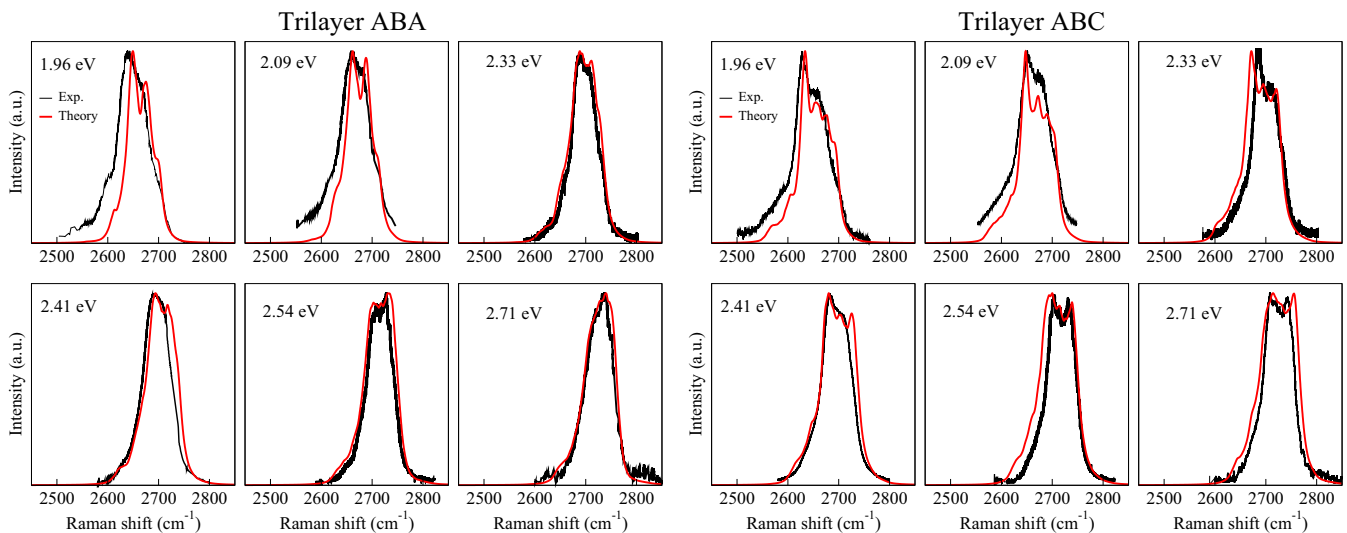


FIG. 2. Measured versus calculated Raman spectra of ABA and ABC trilayer for different laser energies. Experimental data are from Refs. [7,8].

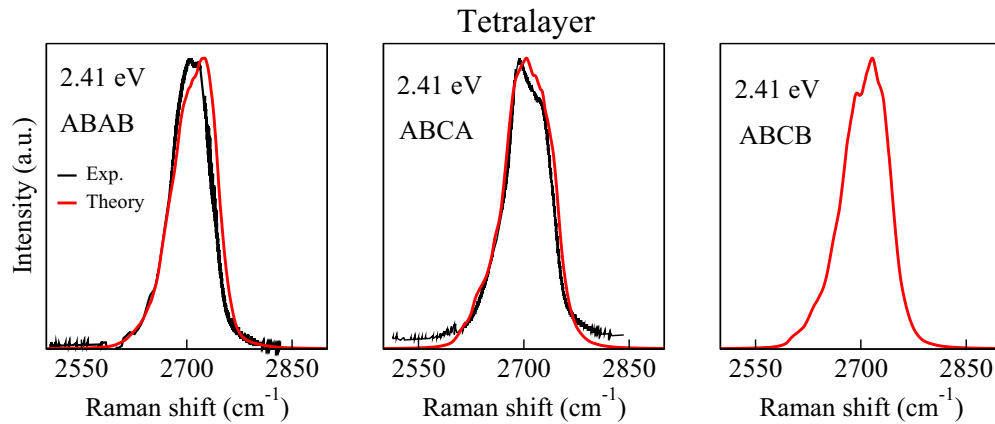


FIG. 3. Measured versus calculated Raman spectra for the three possible stackings in tetralayer graphene at 2.41 eV. Experimental data are from Ref. [7].

stacking. As the bulk ABC structure differs from the bulk ABCB one for the occurrence of long range rhombohedral order, the feature at $\approx 2576 \text{ cm}^{-1}$ at $\omega_L = 1.96 \text{ eV}$ can be seen as a fingerprint of long range rhombohedral order. The good agreement between our theoretical calculation and the experimental spectrum in Ref. [10], both from what concerns the 2D peak width and shape as well as the presence of the feature at $\approx 2576 \text{ cm}^{-1}$ suggests that the samples in Ref. [10] contain long range sequences of rhombohedral stacked multilayer graphene.

It is worthwhile to discuss a bit more the width of the 2D spectra for rhombohedral and Bernal graphite as the larger width of the 2D peak in the former with respect to the latter seems counterintuitive. Indeed, bulk AB-stacked graphite has two couples of π, π^* electronic bands in the BZ, while ABC graphite has only one in the rhombohedral cell. So one could naively think that AB-stacked graphite should have more allowed dipolar transitions. However, this is without taking

into account the electronic k_z dispersion, that, as shown in the Supplemental Material [24], is substantially different along K-M-K in the two case. The different k_z electronic band dispersion implies that different electron and phonon momenta contribute to the Raman cross section. This is clearly seen in Fig. 6 where the resonant phonon momenta contributing to the 2D peak cross sections are highlighted in a contour plot (see also Ref. [16] for more technical explanations). While the Bernal case includes very sharp resonances in phonon momenta, the resonance is much broader in the rhombohedral case due to the different band dispersion along z . This explain the larger width of the 2D peak in the rhombohedral case. More detailed analysis of electronic transitions contributing to the 2D two-phonon resonant cross section are given in the Supplemental Material [24].

In this Rapid Communication we performed parameter-free first principles calculation of the two-phonon resonant 2D and D+D'' peaks in three and four layer graphene for all possible

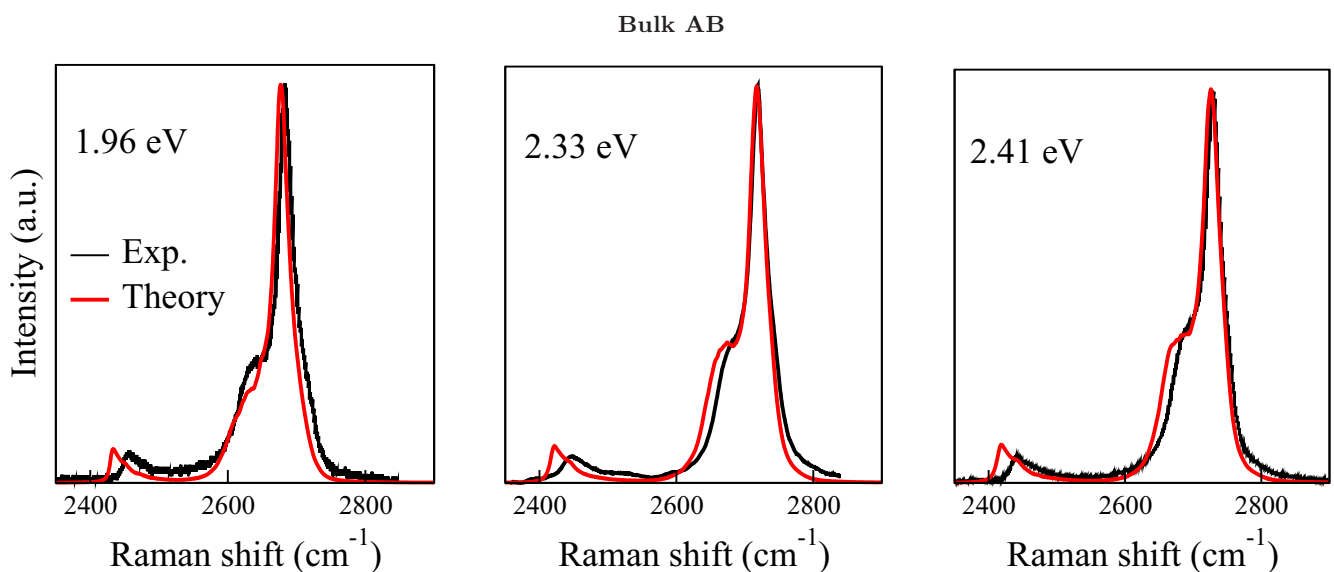


FIG. 4. Comparison between the calculated 2D Raman mode for bulk AB graphite (Bernal graphite) and the experimental Raman spectra obtained from HOPG graphite at different laser energies. Experimental data are from Ref. [21] for 1.96 eV and 2.33 eV and from Ref. [11] for 2.41 eV.

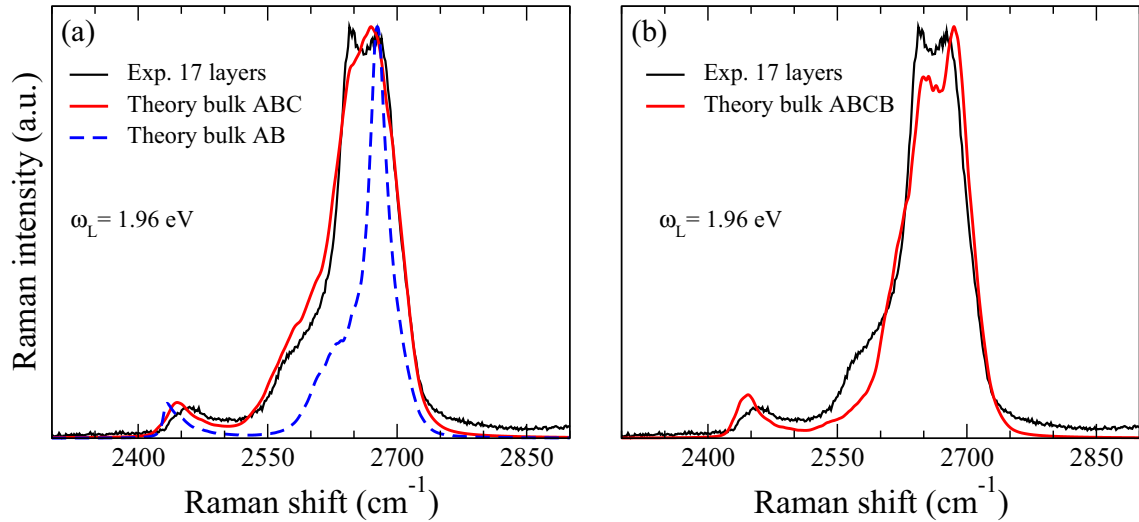


FIG. 5. Theoretical spectra for bulk AB, ABC, and ABCB stacked graphite against experiments at 1.96 eV. (a) The signature of the long range ABC stacking at around $\approx 2576 \text{ cm}^{-1}$ is shown. (b) We show the absence of this signature for short range ABC stacking in ABCB graphite. The experimental data are from samples composed of approximately 17 layers of ABC-stacked graphite [10].

stackings, as well as for bulk AB, ABC, and ABCB graphite, that is a periodic arrangement of AB and ABC graphites. Our calculations carried out for several laser energies are in good agreement with experimental data available for three and four layers with AB and ABC stacking sequences, as well as for Bernal graphite. We found that the fingerprint of long range sequences of ABC-stacked graphene are (i) a broadened 2D peak and (ii) the occurrence of an additional feature at 2576 cm^{-1} for 1.96 eV laser energy. We validate our statement against recently synthesized flakes from Ref. [10] that were tentatively attributed to 17 layers ABC sequences. Our theoretical bulk ABC-stacked graphite spectra confirm this attribution.

A.T. is indebted to the IDS-FunMat European network. M.C. and F.M. acknowledge support from the European Union Horizon 2020 research and innovation programme under Grant agreement No. 696656-GrapheneCore1, PRACE for awarding us access to resource on Marenostrum at BSC and the computer facilities provided by CINES, IDRIS, and CEA TGCC (Grant EDARI No. 2017091202). J.-C.C. acknowledges financial support from the Fédération Wallonie-Bruxelles through the ARC entitled 3D Nanoarchitecturing of 2D crystals (No. 16/21-077), from the European Union's Horizon 2020 researchers and innovation programme (No. 696656), and from the Belgian FNRS.

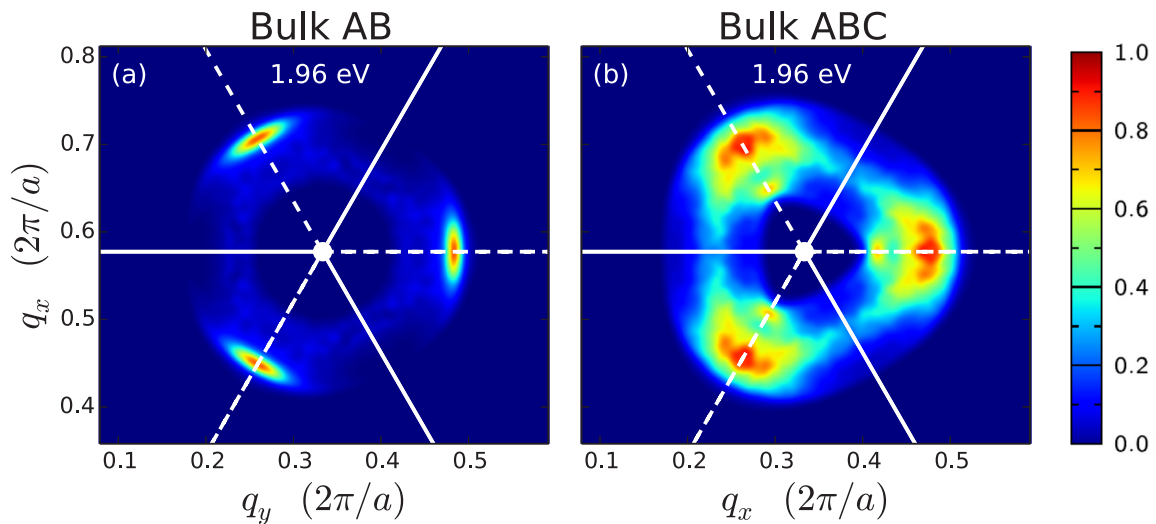


FIG. 6. Phonon momenta contributing to the Raman cross section in bulk AB (a) and bulk ABC (b) graphite around the \mathbf{K} point in the BZ at 1.96 eV. The solid and dashed white lines denote the $\mathbf{K-M}$ and $\mathbf{K-\Gamma}$ high-symmetry lines, respectively. The color bar indicates the normalized \mathbf{q} -resolved Raman cross section, where \mathbf{q} is the phonon momentum. See Supplemental Material [24] for relevant definitions.

- [1] J. D. Bernal, *Proc. Royal Soc. A* **106**, 749 (1924).
- [2] R. Xiao, F. Tasnádi, K. Koepf, J. W. F. Venderbos, M. Richter, and M. Taut, *Phys. Rev. B* **84**, 165404 (2011).
- [3] B. Pamuk, J. Baima, F. Mauri, and M. Calandra, *Phys. Rev. B* **95**, 075422 (2017).
- [4] C. E. Precker, P. D. Esquinazi, A. Champi, J. Barzola-Quiquia, M. Zoraghi, S. Muinos-Landin, A. Setzer, W. Bhlmann, D. Spemann, J. Meijer, T. Muenster, O. Baehre, G. Kloess, and H. Beth, *New J. Phys.* **18**, 113041 (2016).
- [5] J.-C. Charlier, X. Gonze, and J.-P. Michenaud, *Carbon* **32**, 289 (1994).
- [6] K. F. Mak, J. Shan, and T. F. Heinz, *Phys. Rev. Lett.* **104**, 176404 (2010).
- [7] C. H. Lui, Z. Li, Z. Chen, P. V. Klimov, L. E. Brus, and T. F. Heinz, *Nano Lett.* **11**, 164 (2011).
- [8] C. Cong, T. Yu, K. Sato, J. Shang, R. Saito, G. F. Dresselhaus, and M. S. Dresselhaus, *ACS Nano* **5**, 8760 (2011).
- [9] D. Pierucci, H. Sediri, M. Hajlaoui, J. C. Girard, T. Brumme, M. Calandra, E. Velez-Fort, G. Patriarche, M. Silly, G. Ferro *et al.*, *ACS Nano* **9**, 5432 (2015).
- [10] Y. Henni, H. P. Ojeda Collado, K. Nogajewski, M. R. Molas, G. Usaj, C. A. Balseiro, M. Orlita, M. Potemski, and C. Faugeras, *Nano Lett.* **16**, 3710 (2016).
- [11] A. Ferrari, J. Meyer, V. Scardaci, C. Casiraghi, M. Lazzeri, F. Mauri, S. Piscanec, D. Jiang, K. Novoselov, S. Roth *et al.*, *Phys. Rev. Lett.* **97**, 187401 (2006).
- [12] C. Casiraghi, S. Pisana, K. Novoselov, A. Geim, and A. Ferrari, *Appl. Phys. Lett.* **91**, 233108 (2007).
- [13] M. Huang, H. Yan, T. F. Heinz, and J. Hone, *Nano Lett.* **10**, 4074 (2010).
- [14] M. Mohr, J. Maultzsch, and C. Thomsen, *Phys. Rev. B* **82**, 201409 (2010).
- [15] P. May, M. Lazzeri, P. Venezuela, F. Herziger, G. Callsen, J. S. Reparaz, A. Hoffmann, F. Mauri, and J. Maultzsch, *Phys. Rev. B* **87**, 075402 (2013).
- [16] F. Herziger, M. Calandra, P. Gava, P. May, M. Lazzeri, F. Mauri, and J. Maultzsch, *Phys. Rev. Lett.* **113**, 187401 (2014).
- [17] A. C. Ferrari and D. M. Basko, *Nat. Nanotechnol.* **8**, 235 (2013).
- [18] P. Venezuela, M. Lazzeri, and F. Mauri, *Phys. Rev. B* **84**, 035433 (2011).
- [19] D. M. Basko, *Phys. Rev. B* **78**, 125418 (2008).
- [20] V. N. Popov and P. Lambin, *Phys. Rev. B* **87**, 155425 (2013).
- [21] X. Zhang, Q.-H. Tan, J.-B. Wu, W. Shi, and P.-H. Tan, *Nanoscale* **8**, 6435 (2016).
- [22] P. Giannozzi, S. Baroni, N. Bonini, M. Calandra, R. Car, C. Cavazzoni, D. Ceresoli, G. L. Chiarotti, M. Cococcioni, I. Dabo, A. Dal Corso, S. de Gironcoli, S. Fabris, G. Fratesi, R. Gebauer, U. Gerstmann, C. Gougoussis, A. Kokalj, M. Lazzeri, L. Martin-Samos, N. Marzari, F. Mauri, R. Mazzarello, S. Paolini, A. Pasquarello, L. Paulatto, C. Sbraccia, S. Scandolo, G. Sclauzero, A. P. Seitsonen, A. Smogunov, P. Umari, and R. M. Wentzcovitch, *J. Phys.: Condens. Matter* **21**, 395502 (2009).
- [23] M. Calandra, G. Profeta, and F. Mauri, *Phys. Rev. B* **82**, 165111 (2010).
- [24] See Supplemental Material at <http://link.aps.org/supplemental/10.1103/PhysRevMaterials.1.041001> for additional technical details, Raman cross section definition, analysis of the processes contributing to the 2D peak spectrum, polarization analysis, decomposition of the cross section in inner and outer processes and electronic and vibrational properties of graphene multilayer and graphite with and without inclusion of correlation effects.